ISSN 0947-7411, Volume 46, Number 6

Indexed in Current Contents 46 (6) 595–694 (2010)

Heat Mass Transfer (2010) 46:675–686
DOI 10.1007/s00231-010-0602-x

ORIGINAL

Generation of dynamic biochemical signals with a tube mixer: effect of dispersion in an oscillatory flow

K. R. Qin · C. Xiang · S. S. Ge

Received: 9 July 2009 / Accepted: 11 April 2010 / Published online: 22 May 2010

Abstract The generation of controlled dynamic biochemical signals has many applications in the life sciences. This paper presents an analysis of the dispersion of an oscillatory biochemical signal in an incompressible viscous oscillatory flow in a mixing tube. By using the method of Gill and Sankarasubramanian, the dispersion coefficients $K_i(\tau)$ $(i = 1, 2, \ldots)$ are determined as the functions of dimensionless time τ. With the assumptions of quasi-steady flow and steady flow, the dispersion coefficients $K_i(\tau)$ $(i = 1, 2)$ are simplified. The effects of the frequencies of the oscillatory flow and the oscillatory biochemical signal, and the length of the mixing tube on the average solute concentrations, θ_m, over the tube cross-section at the outlet of the mixing tube are analyzed by numerical simulations with and without the assumptions of the quasi-steady and steady flows. It is concluded that for the dispersion in an oscillatory flow, an excellent accuracy can be achieved by using quasi-steady flow assumption while the steady flow assumption would lead to inaccurate results. However, if the frequency of oscillatory flow is sufficiently high, the steady flow assumption can be used to further simplify the calculation while still maintaining sufficient accuracy. These results are of practical importance in producing dynamic biochemical signals as the stimuli of biological cells by a tube mixer.

List of symbols

$Q_1(t)$	Flow rate in the tube (1)
$Q_2(t)$	Flow rate in the tube (2)
$Q(t)$	Flow rate in the tube (3)
Q_m	Non-zero mean of flow rate $Q(t)$
f	frequency of oscillatory flow $Q(t)$
$u(r, t)$	Dimensional velocity along the tube (3)
$\bar{u}(r)$	Steady component of dimensional velocity $u(r, t)$
$\tilde{u}(r)$	Complex amplitude of oscillatory component of dimensional velocity $u(r, t)$
p	Fluid pressure in the tube (3)
r	Radial coordinate in the tube (3)
x	Axial coordinate in the tube (3)
t	Time
C_0	Initial solute concentration in the tube (1)
$C(t, r, x)$	Solute concentration at the coordinate (r, x) at time t
C_m	Non-zero mean of solute concentration $C(t, r, 0)$
f_Ω	Frequency of oscillatory solute concentration $C(t, r, 0)$
D	Molecular diffusivity of ATP
$U(\tau, y)$	Dimensionless velocity along the tube (3)
y	Dimensionless radial coordinate in the tube (3)
X	Dimensionless axial coordinate in the tube (3)
Pe	Péclet number
u_0	Time-averaged dimensional axial velocity along the tube (3)
R	Inner radius of the tube (3)
L	Length of the tube (3)
J_0	Zeroth-order Bessel function
J_1	First-order Bessel function

Greek symbols

ϵ	Dimensionless amplitude of oscillatory component of flow rate $Q(t)$
ω	Angular frequency of flow rate $Q(t)$
ε	Dimensionless amplitude of oscillatory component of solute concentration $C(t, r, 0)$

K. R. Qin · C. Xiang (✉) · S. S. Ge
Department of Electrical and Computer Engineering,
National University of Singapore, Singapore 117576, Singapore
e-mail: elexc@nus.edu.sg

Ω Angular frequency of oscillatory component of solute concentration $C(t, r, 0)$
ϕ Phase of oscillatory component of solute concentration $C(t, r, 0)$
θ_m Dimensionless solute concentration
τ Dimensionless time
μ Dynamic viscosity coefficient of fluid
ρ Fluid density
λ $\lambda^2 = \frac{j^3\rho\omega}{\mu}$, $j = \sqrt{-1}$

1 Introduction

It is well known that dynamic biochemical signals, defined as the time-dependent concentrations of biochemical substances, control biological processes in intra- and intercellular signaling, gene and protein activation and regulate many aspects of cell growth and differentiation [15, 25, 29]. The generation of controlled dynamic biochemical signals has many applications in the life sciences and has received much attention in recent years [4, 10, 19, 24, 31]. In these pioneering works, the waveforms of dynamic biochemical signals have been constructed with microfluidic chips using several schemes [4, 10, 19, 24, 31]. The basic idea in these schemes for producing dynamic biochemical signals is to make the solute from one channel and the solvent from the other channel flow into a mixing micro-channel, defined as a 'mixer'. By controlling the dynamic flow rates of the solute and the solvent at the inlet of the mixing micro-channel, respectively, different kinds of time-dependent biochemical signals can be generated at the outlet of the mixing micro-channel.

While the designs of microfluidic chips are becoming more and more complicated [4, 10, 19, 24, 31], in the past decades, a simple bio-engineering approach, i.e., a parallel-plate flow chamber, in which cultured vascular endothelial cells (ECs) are subjected to both fluid shear stress and biochemical signals by a flow-loading apparatus, has been widely adopted in investigating the mechanism of both fluid shear stress and biochemical stimulation effects on ECs at the cellular and molecular levels [1, 11, 20, 32]. This research focus is motivated by the fact that the ECs in vivo are exposed to both fluid shear stress induced by pulsatile blood flow and biochemical stimuli induced by many biochemical substances. Among the various biochemical stimuli, one of the most important is adenosine triphosphate (ATP)—a ubiquitous extracellular signaling molecule that is related to intracellular calcium dynamics and in turn influences the release of vasodilators such as nitric oxide (NO) and prostacyclin (PGI_2) [1, 11, 20, 26, 32]. In all the previous studies, the ATP signals to which ECs were exposed were time-invariant while the fluid shear stresses were sometimes time-varying. However, the ECs in vivo are stimulated simultaneously by both dynamic fluid shear stress and dynamic biochemical signals. In order to design the experiments to investigate the effects of both dynamic fluid shear stress and dynamic biochemical signals on ECs cultured at the bottom of the flow chamber, a tube mixer as shown in Fig. 1 should be connected to the inlet of the flow chamber so as to simultaneously produce both dynamic flows and dynamic biochemical signals in the flow chamber.

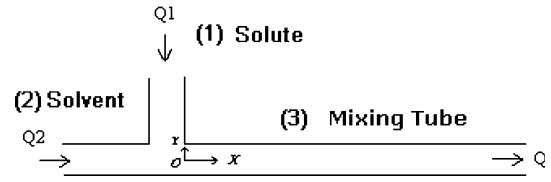

Fig. 1 A sketch of the tube mixer

For the tube mixer, suppose the walls of the tubes are rigid, the flow rates in the tube (1)–(3) are the functions of time t, $Q_1(t)$, $Q_2(t)$ and $Q(t)$, respectively. The continuity of incompressible flow tells us

$$Q_1(t) + Q_2(t) = Q(t). \tag{1}$$

It is assumed that the solute dispersion near the junction of the tube mixer is ignored, and the distribution of the solute is uniform across the tube cross-section at $x = 0$ along x-direction of the tube (3). Thus, the concentration, $C(t, r, 0)$, of the solute at the inlet of the mixing tube (3) satisfying mass conservation law is expressed as

$$C_0 Q_1(t) = C(t, r, 0)Q(t), \tag{2}$$

where r is the radial coordinate, C_0 is the initial concentration of the solute in the tube (1) and is a constant. By using Eqs. 1 and 2, the expressions of the flow rates $Q_1(t)$ and $Q_2(t)$ are given by

$$Q_1(t) = \frac{C(t, r, 0)Q(t)}{C_0}, \tag{3}$$

and

$$Q_2(t) = Q(t)\left(1 - \frac{C(t, r, 0)}{C_0}\right), \tag{4}$$

which means that given initial solute concentration C_0, in order to obtain any desired flow rate $Q(t)$ and any desired solute concentration $C(t, r, 0)$ at the inlet of the tube (3), we just need to set the values of the flow rates $Q_1(t)$ and $Q_2(t)$ by Eqs. 3 and 4. Obviously, the flow rate $Q(t)$ can be a constant or time-dependent, i.e., the laminar flow in the tube (3) can be steady or time-dependent, and the flow rate $Q(t)$ and the concentration $C(t, r, 0)$ can be set up independently.

In practice, the tube (3) is quite long so that the effect of the solute dispersion in the tube (3) should be considered to get correct biochemical dynamic signals at the outlet of the tube (3). It was first shown by Taylor [28] that when a passive solute is introduced into a fluid moving slowly and steadily through a circular tube, the eventual dispersion of the solute is enhanced by the flow of the fluid. Since then, there exist a large number of studies on dispersion of inert matter in the steady flows and time-dependent flows in channels or tubes, some classical works may include Aris [2, 3], Gill and Sankarasubramanian [12–14], Chatwin [8, 9], Smith [27] and Yasuda [33], etc. Some more recent developments may include Mukherjee and Mazumder [21], Jiang and Grotberg [18], Hazra et al. [16, 17], Bandyopadhyay and Mazumder [5, 6], Ng [22] and so on. By taking the dispersion into consideration in the problem for generating dynamic biochemical signals, it was first shown by Mastrangelo and his colleagues that long mixing channels in the micro-mixers in the micro-fuidic chips acted as low-pass filters that reduced the amplitudes of the biochemical waves at the outlets moving from the inlets and cut off the high frequency components of these biochemical waves [4, 10, 31]. However, only the solute dispersion in a steady flow in the mixing channel was considered in the design of their microfluidic chips [4, 10, 31]. If the flow in a mixing channel or tube is time-dependent, the effect of dispersion in a time-dependent laminar flow has to be considered.

The aim of this paper is to analyze the dispersion of oscillatory solute in an oscillatory laminar flow in the mixing tube. First, the longitudinal dispersion coefficients, $K_i(\tau)$ ($i = 1, 2, \ldots$), of an oscillatory solute in an oscillatory viscous incompressible laminar flow in the mixing tube are determined as functions of dimensionless time τ by the technique of Gill and Sankarasubramanian [12–14]. Under the assumptions of the quasi-steady flow and steady flow, the dispersion coefficients, $K_i(\tau)$ ($i = 1, 2$), are also simplified as the functions of dimensionless time τ. Then, θ_m, the dimensionless average concentration of the solute over the tube cross-section at the outlet of the mixing tube, i.e., the desired dynamic biochemical signal, is determined as function of dimensionless time τ with or without the assumptions of the quasi-steady flow and steady flow. Finally, the effects of the frequencies of oscillatory flow and oscillatory solute concentration at the inlet, and the length of the mixing tube on the dynamic biochemical signal at the outlet are analyzed by numerical simulation studies with or without the assumptions of the quasi-steady flow and steady flow.

2 Dispersion in an oscillatory laminar flow in a mixing tube

2.1 Problem formulation and solutions

Consider the dispersion of an oscillating solute in an oscillatory laminar flow of an incompressible viscous fluid in a straight circular mixing tube as shown in Fig. 1.

According to the introduction in Sect. 1, the flow rate $Q(t)$ and the solute concentration $C(t, r, 0)$ can be set up independently. Suppose the oscillatory flow rate $Q(t)$ in the tube (3) is expressed as

$$Q(t) = Q_m(1 + \epsilon \cos \omega t), \tag{5}$$

where Q_m is the non-zero mean of flow rate $Q(t)$, $Q_m\epsilon$ is the amplitude of oscillation with angular frequency ω satisfying $\omega = 2\pi f$, f is the frequency of oscillatory flow, and the concentration $C(t, r, 0)$ of oscillatory solute at the inlet of the tube (3) is given by

$$C(t, r, 0) = C_m[1 + \varepsilon \cos(\Omega t + \phi)], \tag{6}$$

where C_m is the non-zero mean of the concentration $C(t, r, 0)$, $C_m\varepsilon$ is the amplitude of oscillation with angular frequency Ω satisfying $\Omega = 2\pi f_\Omega$, f_Ω is the frequency of oscillatory solute, ϕ is the phase of the oscillation.

To satisfy Eqs. 5 and 6, the flow rates $Q_1(t)$ and $Q_2(t)$ by Eqs. 3 and 4 should satisfy

$$Q_1(t) = \frac{Q_m C_m}{C_0}(1 + \epsilon \cos \omega t)[1 + \varepsilon \cos(\Omega t + \phi)] \tag{7}$$

and

$$Q_2(t) = Q_m(1 + \epsilon \cos \omega t)\left(1 - \frac{C_m}{C_0}[1 + \varepsilon \cos(\Omega t + \phi)]\right), \tag{8}$$

respectively.

It is assumed that the effect of the junction of the tube mixer is ignored so that the flow in the mixing tube (3) is fully developed axisymmetric flow. Under this assumption, the axial velocity $u(r, t)$ along x-direction in tube (3) satisfies the Navier–Stokes equation which can be simplified as follows [7, 23, 30]

$$\frac{\partial u}{\partial t} = -\frac{1}{\rho}\frac{\partial p}{\partial x} + \frac{\mu}{\rho}\frac{1}{r}\frac{\partial}{\partial r}\left(r\frac{\partial u}{\partial r}\right), \tag{9}$$

where $\frac{\partial p}{\partial x}$ is the axial pressure gradient, ρ is the fluid density, μ is the viscosity. By solving the equation [7, 23, 30], the velocity profile in terms of the steady and oscillatory components of the flow rate is given by Cegeaux and Grondelle [7]

$$u(r, t) = \bar{u}(r) + Re(\tilde{u}(r)e^{j\omega t}), \tag{10}$$

where

$$\bar{u}(r) = \frac{2Q_m}{\pi R^2}\left(1 - \frac{r^2}{R^2}\right), \tag{11}$$

is the steady component of the velocity (where the overbar denotes time averaging over a period of oscillation, R is the inner radius of the tube), and

$$\tilde{u}(r) = \frac{Q_m \epsilon}{\pi R^2}\left[\frac{1 - \frac{J_0(r\lambda)}{J_0(R\lambda)}}{1 - F_{10}}\right], \tag{12}$$

is the complex amplitude of the oscillatory component of the fluid velocity. In the equation above,

$$\lambda^2 = \frac{j^3 \rho \omega}{\mu}, \quad F_{10} = \frac{2J_1(\lambda R)}{\lambda R J_0(\lambda R)}, \tag{13}$$

where J_0 and J_1 are the zeroth-order and first-order Bessel functions of the first kind, respectively.

The convective diffusion equation which describes the local concentration, C, of solute as a function of axial distance x, radial distance r and time t for time variable flow in a straight circular tube is [3]

$$\frac{\partial C}{\partial t} + u(r,t)\frac{\partial C}{\partial x} = D\left[\frac{1}{r}\frac{\partial}{\partial r}\left(r\frac{\partial C}{\partial r}\right) + \frac{\partial^2 C}{\partial x^2}\right], \tag{14}$$

where D is the diffusion coefficient.

When $x \to +\infty$, the concentration gradient along x-direction satisfies

$$\frac{\partial C(t,r,+\infty)}{\partial x} \to 0, \tag{15}$$

The boundary conditions at r-direction may be written as

$$\frac{\partial C(t,0,x)}{\partial r} = \frac{\partial C(t,R,x)}{\partial r} = 0, \tag{16}$$

The initial conditions are

$$C(t,r,0) = C_m(1 + \varepsilon \cos\phi), \tag{17}$$

Let us introduce the dimensionless quantities

$$\theta = \frac{C}{C_0}, \quad U(\tau,y) = \frac{u(r,t)}{u_0}, \quad X = \frac{Dx}{R^2 u_0}, \tag{18}$$

$$Pe = \frac{u_0 R}{D}, \quad \tau = \frac{Dt}{R^2}, \quad y = \frac{r}{R}, \tag{19}$$

where u_0 is the time-averaged axial velocity on the central line $r = 0$ given by

$$u_0 = \frac{\omega}{2\pi}\int_0^{\frac{2\pi}{\omega}} u(0,t)dt = \frac{2Q_m}{\pi R^2}, \tag{20}$$

where $2\pi/\omega$ is the period of the pulsating flow rate given by (1). Using (18) and (19) in (14)–(16) gives

$$\frac{\partial \theta}{\partial \tau} + U(\tau,y)\frac{\partial \theta}{\partial X} = \frac{1}{y}\frac{\partial}{\partial y}y\frac{\partial \theta}{\partial y} + \frac{1}{(Pe)^2}\frac{\partial^2 \theta}{\partial X^2}, \tag{21}$$

subject to the boundary conditions

$$\theta(\tau,y,0) = 1 + \varepsilon \cos\left(\frac{R^2\Omega}{D}\tau + \phi\right), \tag{22}$$

$$\frac{\partial \theta(\tau,y,+\infty)}{\partial X} \to 0, \tag{23}$$

$$\frac{\partial \theta(\tau,0,X)}{\partial y} = \frac{\partial \theta(\tau,1,X)}{\partial y} = 0, \tag{24}$$

and the initial conditions

$$\theta(0,y,X) = 1 + \varepsilon \cos\phi. \tag{25}$$

Following Gill and Sankarasubramanian [13], the solution of (21) subject to (22)–(24) is formulated as

$$\theta(\tau,y,X) = \sum_{k=0}^{\infty} f_k(\tau,y)\frac{\partial^k \theta_m}{\partial X^k}, \tag{26}$$

where

$$\theta_m = 2\int_0^1 \theta y dy. \tag{27}$$

Substitution of (26) in (21) gives

$$\sum_{k=0}^{\infty}\left[\left(\frac{\partial f_k}{\partial \tau} - \frac{1}{y}\frac{\partial}{\partial y}y\frac{\partial f_k}{\partial y}\right)\frac{\partial^k \theta_m}{\partial X^k} + U(\tau,y)f_k\frac{\partial^{k+1}\theta_m}{\partial X^{k+1}} - \frac{1}{(Pe)^2}f_k\frac{\partial^{k+2}\theta_m}{\partial X^{k+2}} + f_k\frac{\partial^{k+1}\theta_m}{\partial \tau \partial X^k}\right] = 0. \tag{28}$$

By using (27), integration of (21) gives

$$\frac{\partial \theta_m}{\partial \tau} = \frac{1}{(Pe)^2}\frac{\partial^2 \theta_m}{\partial X^2} - 2\int_0^1 yU(\tau,y)\frac{\partial \theta}{\partial X}dy. \tag{29}$$

Using (27) in (29) leads to

$$\frac{\partial \theta_m}{\partial \tau} = \sum_{i=1}^{\infty} K_i(\tau)\frac{\partial^i \theta_m}{\partial X_i}, \tag{30}$$

where

$$K_1(\tau) = -2\int_0^1 U(\tau,y)f_0(\tau,y)ydy, \tag{31}$$

$$K_2(\tau) = \frac{1}{(Pe)^2} - 2\int_0^1 U(\tau,y)f_1(\tau,y)ydy, \tag{32}$$

$\vdots$

$$K_{i+2}(\tau) = -2\int_0^1 U(\tau,y) f_{i+1}(\tau,y) y dy \quad (i = 1,2,3,\ldots). \tag{33}$$

By substituting (30) in (28) and equating the coefficients of $\partial^k\theta_m/\partial X^k$, the equations for $f_k(\tau, y)$ are obtained as follows

$$\frac{\partial f_0}{\partial \tau} = \frac{1}{y}\frac{\partial}{\partial y} y \frac{\partial f_0}{\partial y}, \tag{34}$$

$$\frac{\partial f_1}{\partial \tau} = \frac{1}{y}\frac{\partial}{\partial y} y \frac{\partial f_1}{\partial y} - [U(\tau,y) + K_1(\tau)] f_0, \tag{35}$$

$$\frac{\partial f_2}{\partial \tau} = \frac{1}{y}\frac{\partial}{\partial y} y \frac{\partial f_2}{\partial y} + \left[\frac{1}{(Pe)^2} - K_2(\tau)\right] f_0 - [U(\tau,y) + K_1(\tau)] f_1, \tag{36}$$

$$\vdots$$

$$\frac{\partial f_k}{\partial \tau} = \frac{1}{y}\frac{\partial}{\partial y} y \frac{\partial f_k}{\partial y} - [U(\tau,y) + K_1(\tau)] f_{k-1} + \left[\frac{1}{(Pe)^2} - K_2(\tau)\right] f_{k-2} - \sum_{i=3}^{k} K_i f_{k-i} \quad (k = 3,4,\ldots). \tag{37}$$

Equations 22, 23, 25 and 27 give

$$\theta_m(\tau,0) = 1 + \varepsilon \cos\left(\frac{R^2\Omega}{D}\tau + \phi\right), \tag{38}$$

$$\frac{\partial \theta_m(\tau,+\infty)}{\partial X} \to 0, \tag{39}$$

$$\theta_m(0,X) = 1 + \varepsilon\cos\phi. \tag{40}$$

Now from (26), the initial conditions for f_k can be taken as

$$f_0(0,y) = 1, \quad f_k(0,y) = 0, \quad \text{for } k = 1,2,3,\ldots \tag{41}$$

Similarly the boundary conditions for f_k are derived from (24) and (26) as

$$\frac{\partial f_k(\tau,0)}{\partial y} = \frac{\partial f_k(\tau,1)}{\partial y} = 0 \quad (k = 0,1,2,\ldots). \tag{42}$$

Further Eqs. 26 and 27 are consistent if

$$\int_0^1 f_0 y dy = \frac{1}{2}, \quad \int_0^1 f_k y dy = 0, \quad \text{for } k = 1,2,3,\ldots \tag{43}$$

With the initial and boundary conditions given by (41)–(43), the functions $f_k(\tau, y)$ can be determined by solving the system of Eqs. 31–33 and then the dispersion coefficients $K_i(\tau)$ can be obtained from (34) to (37).

By using (18) and (19), the dimensionless velocity profile can be derived from (10) to (12) as follows

$$U(\tau,y) = 1 - y^2 + \frac{\epsilon}{2} Re\left(\frac{1 - \frac{J_0(y\lambda R)}{J_0(\lambda R)}}{1 - F_{10}} e^{j\xi^2\tau}\right), \tag{44}$$

where

$$\xi^2 = \frac{R^2\omega}{D}. \tag{45}$$

It can be readily shown that the solution of (34) subject to (41)–(43) is given by

$$f_0(\tau,y) \equiv 1. \tag{46}$$

Substitution of (44) and (46) in (31) then gives

$$K_1(\tau) = -\frac{1}{2}\left(1 + \epsilon\cos(\xi^2\tau)\right). \tag{47}$$

The differential equation for f_1 is

$$\frac{\partial f_1}{\partial \tau} = \frac{1}{y}\frac{\partial}{\partial y} y \frac{\partial f_1}{\partial y} - \left[1 - y^2 + \frac{\epsilon}{2} Re\left(\frac{1 - \frac{J_0(y\lambda R)}{J_0(\lambda R)}}{1 - F_{10}} e^{j\xi^2\tau}\right) - \frac{1}{2}\left(1 + \epsilon\cos(\xi^2\tau)\right)\right]. \tag{48}$$

This is to be solved with the conditions

$$f_1(0,y) = 0, \quad \left.\frac{\partial f_1}{\partial y}\right|_{y=0} = \left.\frac{\partial f_1}{\partial y}\right|_{y=1}. \tag{49}$$

From Duhamel's theorem, it follows that

$$f_1(\tau,y) = \frac{\partial}{\partial \tau}\int_0^\tau F(\tau - \zeta, y; \zeta) d\zeta \tag{50}$$

provided $F(\tau, y;\zeta)$ satisfies

$$\frac{\partial F}{\partial \tau} = \frac{1}{y}\frac{\partial}{\partial y} y \frac{\partial F}{\partial y} - \left[1 - y^2 + \frac{\epsilon}{2} Re\left(\frac{1 - \frac{J_0(y\lambda R)}{J_0(\lambda R)}}{1 - F_{10}} e^{j\xi^2\zeta}\right) - \frac{1}{2}\left(1 + \epsilon\cos(\xi^2\zeta)\right)\right], \tag{51}$$

subject to

$$F(0,y;\zeta) = 0, \quad \left.\frac{\partial F}{\partial y}\right|_{y=0} = \left.\frac{\partial F}{\partial y}\right|_{y=1} = 0, \quad \int_0^1 F y dy = 0. \tag{52}$$

Note that ζ behaves like a parameter while solving (51). Equation 51 subject to (52) may be solved by straightforward methods upon separating F into steady-state and transient parts. The final result is

$$F(\tau,y;\zeta)=\frac{1}{4}y^2-\frac{1}{16}y^4-\frac{1}{8}y^2(1+\epsilon\cos(\xi^2\zeta))+\frac{\epsilon}{2}Re\left(\frac{\frac{1}{4}y^2+\frac{J_0(y\lambda R)}{(\lambda R)^2J_0(\lambda R)}}{1-F_{10}}e^{j\xi^2\zeta}\right)+\sum_{n=0}^{\infty}A_ne^{-\alpha_n^2\tau}J_0(\alpha_ny) \quad (53)$$

where α_n's are defined by $J_1(\alpha_n)=0$, A_0 and A_n satisfy

$$A_0=-\frac{1}{24}+\frac{1}{16}\epsilon\cos(\xi^2\zeta)-\frac{\epsilon}{2}Re\left(\frac{\frac{1}{8}+\frac{F_{10}}{(\lambda R)^2}}{1-F_{10}}e^{j\xi^2\zeta}\right),$$

$$A_n=\frac{1}{J_0(\alpha_n)}\left[-\frac{4}{\alpha_n^4}+\frac{\epsilon}{2}Re\left(\frac{(\lambda R)^2}{\alpha_n^2(\alpha_n^2-(\lambda R)^2)}\frac{F_{10}}{1-F_{10}}e^{j\xi^2\zeta}\right)\right]\quad(n=1,2,3\ldots) \quad (54)$$

Equations 50 and 53 now give

$$f_1(\tau,y)=-\frac{1}{24}+\frac{1}{8}y^2-\frac{1}{16}y^4+\left(\frac{1}{16}-\frac{1}{8}y^2\right)\epsilon\cos(\xi^2\tau)+\frac{\epsilon}{2}Re\left(\frac{-\frac{1}{8}+\frac{1}{4}y^2-\frac{F_{10}}{(\lambda R)^2}+\frac{J_0(y\lambda R)}{(\lambda R)^2J_0(\lambda R)}}{1-F_{10}}e^{j\xi^2\tau}\right)+Re\sum_{n=1}^{\infty}\left[\left(-\frac{4}{\alpha_n^4}e^{-\alpha_n^2\tau}+\frac{\epsilon}{2}\frac{(\lambda R)^2}{\alpha_n^2(\alpha_n^2-(\lambda R)^2)}\frac{F_{10}}{1-F_{10}}\times\frac{j\xi^2e^{j\xi^2\tau}+\alpha_n^2e^{-\alpha_n^2\tau}}{j\xi^2+\alpha_n^2}\right)\frac{J_0(\alpha_ny)}{J_0(\alpha_n)}\right]. \quad (55)$$

Substituting the real part of $U(\tau, y)$ from (44) and the real part of $f_1(\tau, y)$ from (55) in (32), we get the dispersion coefficient $K_2(\tau)$ as follows

$$K_2(\tau)=\frac{1}{(Pe)^2}+\frac{1}{192}+D_2(\tau). \quad (56)$$

where $D_2(\tau)$ represents the time-dependent part of the dispersion coefficient. However, the expression for $D_2(\tau)$, being extremely complicated, is omitted. With $U(\tau, y)$, $f_0(\tau, y)$, $K_1(\tau)$, $f_1(\tau, y)$ and $K_2(\tau)$ known, the expression for $f_2(\tau, y)$ can be solved from (36). After determining $f_2(\tau, y)$, K_3 can then be computed from (33) by putting $i = 1$. This process can be repeated to determine the higher order dispersion coefficients K_4, K_5,.... However, it is shown for the problems of convective diffusion in a steady flow in [12] that K_3, K_4, K_5,... are much smaller than K_2. Thus to a good approximation, Eq. 30 can be written as

$$\frac{\partial\theta_m}{\partial\tau}=K_1(\tau)\frac{\partial\theta_m}{\partial X}+K_2(\tau)\frac{\partial^2\theta_m}{\partial X^2} \quad (57)$$

subject to the initial and boundary conditions (38)–(40).

2.2 Quasi-steady and steady flow assumptions

Suppose that Womersley number [30] $\alpha=R\sqrt{\frac{\rho\omega}{\mu}}$ is quite small in the oscillatory flow in the mixing tube, the dimensionless velocity profile can be simplified by quasi-steady flow assumption as

$$U(\tau,y)=(1-y^2)\left(1+\epsilon\cos(\xi^2\tau)\right), \quad (58)$$

Hence, Eq. 55 can be simplified as

$$f_1(\tau,y)=\left(-\frac{1}{24}+\frac{1}{8}y^2-\frac{1}{16}y^4\right)\left(1+\epsilon\cos(\xi^2\tau)\right)-Re\sum_{n=1}^{\infty}\left[\frac{4}{\alpha_n^4}\frac{J_0(\alpha_ny)}{J_0(\alpha_n)}\left(e^{-\alpha_n^2\tau}+\epsilon\frac{j\xi^2e^{j\xi^2\tau}+\alpha_n^2e^{-\alpha_n^2\tau}}{j\xi^2+\alpha_n^2}\right)\right]. \quad (59)$$

Substituting $U(\tau, y)$ from (58) and $f_1(\tau, y)$ from (59) in (32), we get the dispersion coefficient $K_2(\tau)$ with quasi-steady flow assumption as follows

$$K_2(\tau)=\frac{1}{(Pe)^2}+\frac{1}{192}\left(1+\epsilon\cos(\xi^2\tau)\right)^2-\sum_{n=1}^{\infty}\left[\frac{16}{\alpha_n^6}\left(1+\epsilon\cos(\xi^2\tau)\right)\left(e^{-\alpha_n^2\tau}+\epsilon\frac{j\xi^2e^{j\xi^2\tau}+\alpha_n^2e^{-\alpha_n^2\tau}}{j\xi^2+\alpha_n^2}\right)\right]. \quad (60)$$

The expression of the dispersion coefficient $K_1(\tau)$ with quasi-steady flow assumption is the same as Eq. 47.

Under the assumption of steady flow in the mixing tube, we have

$$K_1(\tau)=-\frac{1}{2}, \quad (61)$$

$$K_2(\tau)=\frac{1}{(Pe)^2}+\frac{1}{192}-\sum_{n=1}^{\infty}\frac{16}{\alpha_n^6}e^{-\alpha_n^2\tau}. \quad (62)$$

As $\tau\longrightarrow\infty$, the coefficient K_2 is expressed as

$$K_2(\tau)=\frac{1}{(Pe)^2}+\frac{1}{192}, \quad (63)$$

which was given by Aris [2].

2.3 Model parameter values and numerical simulations

For the purpose of numerical simulations, all the values for model parameters are required. Table 1 summarizes the values for these parameters used in the numerical simulations.

For the dispersion in an oscillatory flow, by using Eqs. 32, 44, 47 and 55, the dispersion coefficients $K_1(\tau)$ and $K_2(\tau)$ are calculated. In order to test the accuracy of quasi-steady flow assumption, the dispersion coefficients $K_1(\tau)$ and $K_2(\tau)$ are computed by using the Eqs. 47 and 60.

Table 1 Parameter values for numerical simulations

Parameter	Unit	Value
R	m	9×10^{-4}
L	m	0.1–0.5
μ	Pa s	0.001
ρ	kg m^{-3}	1.0×10^{3}
D	m^2 s^{-1}	2.36×10^{-10}
ϵ		0.5
f	Hz	0.02–1.0
ε		0.5
f_Ω	Hz	0.02–1.0
ϕ		0

It would be interesting to see whether the steady flow assumption can be used to further simplify the calculation while still maintaining sufficient accuracy. For this purpose, the dispersion coefficients $K_1(\tau)$ and $K_2(\tau)$ are also determined by using Eqs. 61 and 62.

After the dispersion coefficients $K_1(\tau)$ and $K_2(\tau)$ in the oscillatory flow being obtained, as well as under the assumptions of quasi-steady and steady flows, Eq. 57 can be solved numerically by finite difference schema using the initial and boundary conditions (38)–(40). The computer code developed for this purpose is based on a backward Euler formulation in τ direction with the central difference approximations of the first and second derivatives of θ_m in X direction. Finally, the dimensionless average solute concentrations, θ_m, at the outlet of the mixing tube (3), i.e., the desired dynamic solute signals, are then determined as functions of dimensionless time τ in the oscillatory flow, and under the assumptions of quasi-steady and steady flows.

In the numerical simulations, the effects of the frequencies of oscillatory flow $Q(t)$ and oscillatory solute concentration $C(t, r, 0)$, and the length of the mixing tube (3) on the solute dispersions are carefully considered. Without loss of generality, the amplitude ϵ of oscillatory component of $Q(t)$, the amplitude ε and the phase ϕ of oscillatory component of $C(t, r, 0)$ are fixed to be 0.5, 0.5 and 0, respectively.

3 Numerical results

3.1 Dispersion coefficients K_1 and K_2 in an oscillatory flow

Figures 2 and 3 show the dispersion coefficients K_i $(i = 1, 2)$ versus dimensionless time τ in the oscillatory flow (solid line) with different frequencies 1 Hz (a), 0.2 Hz (b), 0.04 Hz (c) and 0.02 Hz (d), and those under the assumptions of

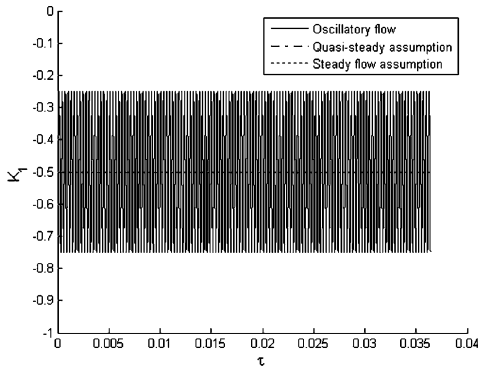

(a) $f = 1Hz$

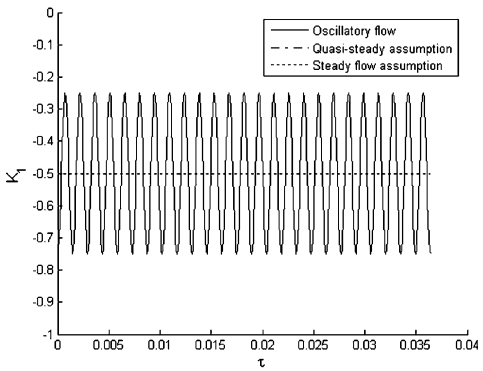

(b) $f = 0.2Hz$

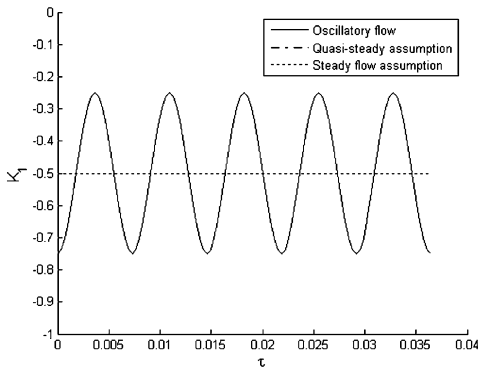

(c) $f = 0.04Hz$

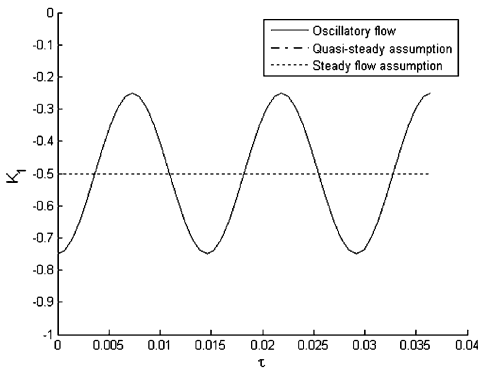

(d) $f = 0.02Hz$

Fig. 2 Plot of the dispersion coefficient K_1 as a function of dimensionless time τ

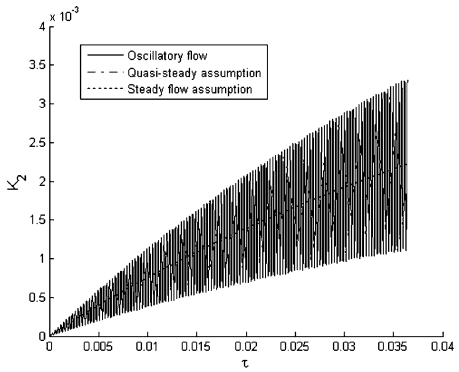

(a) $f = 1Hz$

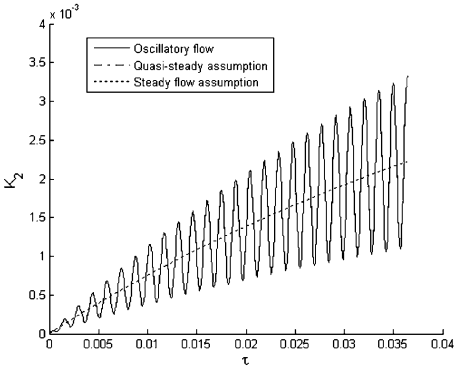

(b) $f = 0.2Hz$

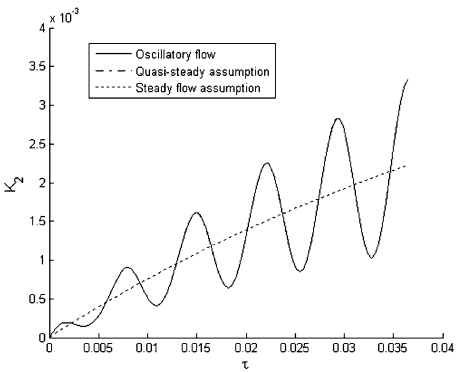

(c) $f = 0.04Hz$

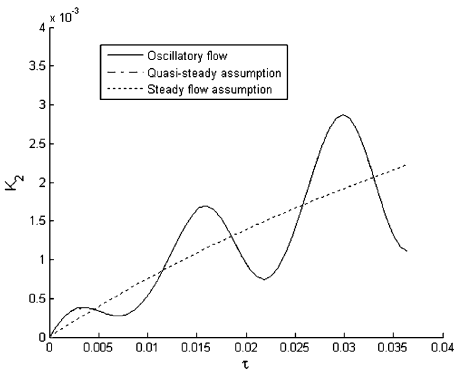

(d) $f = 0.02Hz$

Fig. 3 Plot of the dispersion coefficient K_2 as a function of dimensionless time τ

quasi-steady flow (dash-dotted line) and steady flow (dotted line). It is seen that the dispersion coefficients K_i ($i = 1, 2$) determined by using quasi-steady flow assumption have almost the same values as those calculated by using the original expressions in the oscillatory flow, the dispersion coefficients K_i ($i = 1, 2$) in the oscillatory flow have extra oscillating components in comparison with those under the steady flow assumption, and the oscillatory frequency of K_i ($i = 1, 2$) decreases with the frequency of the oscillatory flow.

3.2 Effect of the frequency of oscillatory flow on the solute dispersion

In order to investigate the effect of the frequency of oscillatory flow on the solute dispersion, the frequency of oscillatory solute concentration is fixed to 0.04 Hz but the frequency of oscillatory flow is changed from 1 to 0.02 Hz in the numerical simulations. Figure 4 shows the dimensionless average concentration θ_m versus dimensionless time τ at the outlet of the mixing tube with the length 0.4 m, i.e., the desired dynamic solute signals, when the frequency of the oscillatory flow (dashed line) is 1 Hz (a), 0.2 Hz (b), 0.05 Hz (c) and 0.02 Hz (d), respectively. It can be seen that the desired dynamic solute signals at the outlet of the mixing tube under quasi-steady flow assumption (dash-dotted line) are almost the same as those in the oscillatory flow (dashed line). However, it is evident that if the frequencies of oscillatory flows are as high as 1 Hz (a) and 0.2 Hz (b), the desired dynamic solute signals under the assumptions of quasi-steady flow (dash-dotted line) and steady flow (dotted line) are almost the same as those in the oscillatory flow (dashed line),but if the frequencies of oscillatory flows are as low as 0.05 Hz (c) and 0.02 Hz (d), the desired dynamic biochemical signals under the steady flow assumption(dotted line) are different from those in the oscillatory flow (dashed line) and under the quasi-steady flow assumption (dash-dotted line). It is concluded that the steady assumption can be used only for the calculation of the desired dynamic solute signals when the frequency of oscillatory flow is sufficiently high.

3.3 Effect of the frequency of oscillatory solute concentration on the solute dispersion

In order to investigate the effect of the frequency of oscillatory solute concentration on the solute dispersion, the frequency of oscillatory flow is fixed to 0.04 Hz but the frequency of oscillatory solute concentration is changed from 1 to 0.02 Hz in the numerical simulations. Figure 5 shows the dimensionless average concentration θ_m versus dimensionless time τ at the outlet of the mixing tube with the length 0.4 m when the frequency of the oscillatory

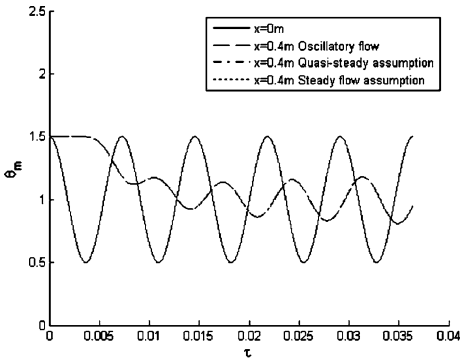

(a) $f = 1Hz$ and $f_\Omega = 0.04Hz$

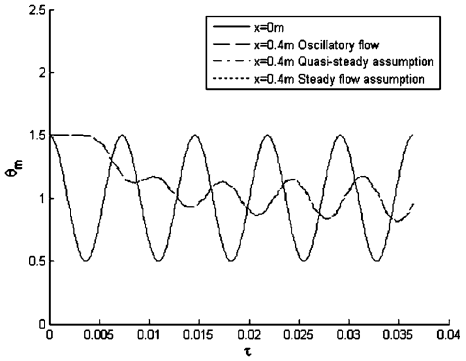

(b) $f = 0.2Hz$ and $f_\Omega = 0.04Hz$

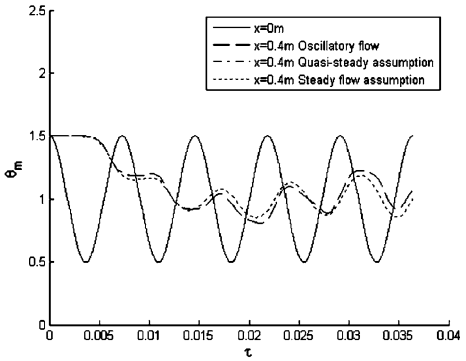

(c) $f = 0.05Hz$ and $f_\Omega = 0.04Hz$

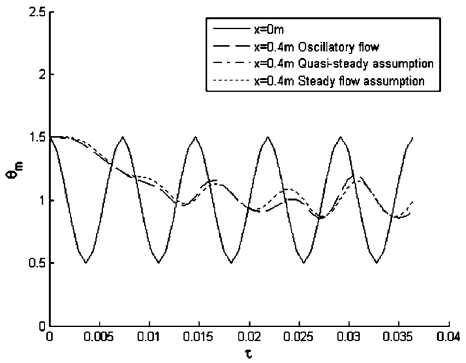

(d) $f = 0.02Hz$ and $f_\Omega = 0.04Hz$

Fig. 4 Effect of the frequency of oscillatory flow on the dimensionless average concentration θ_m versus dimensionless time τ at $x = 0.4$ m

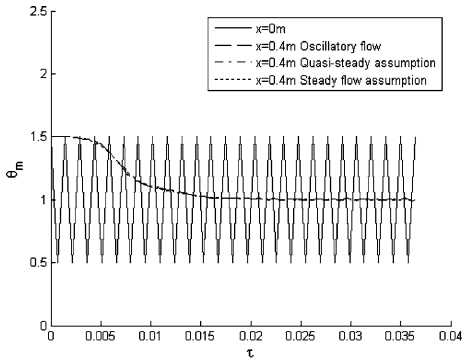

(a) $f = 0.04Hz$ and $f_\Omega = 1Hz$

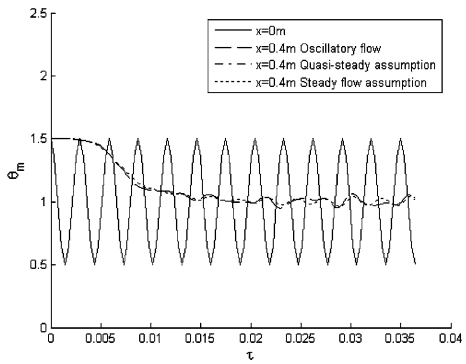

(b) $f = 0.04Hz$ and $f_\Omega = 0.1Hz$

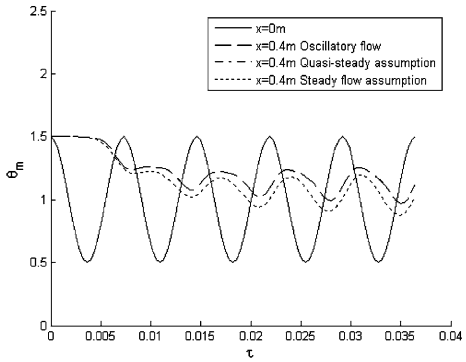

(c) $f = 0.04Hz$ and $f_\Omega = 0.04Hz$

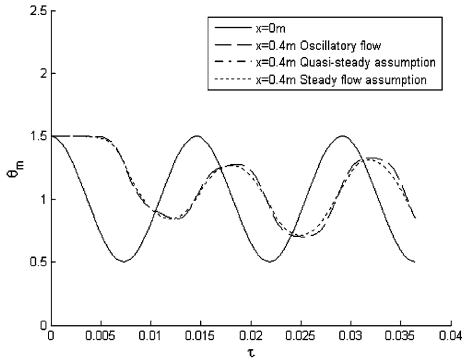

(d) $f = 0.04Hz$ and $f_\Omega = 0.02Hz$

Fig. 5 Effect of the frequency of oscillatory solute concentration on the dimensionless average concentration θ_m versus dimensionless time τ at $x = 0.4$ m

solute concentration is 1 Hz (a), 0.1 Hz (b), 0.04 Hz (c) and 0.02 Hz (d), respectively. It can be easily seen that the frequency of oscillatory solute concentration will significantly affect the solute dispersion in the oscillatory flow so that the desired dynamic solute signals at the outlet of the mixing tube have much more decay with increases in the frequency of oscillatory solute concentration. It is also worth noting that if the frequency of oscillatory solute concentration is as high as 1 Hz (a), the oscillation of desired dynamic solute signal at the outlet of the mixing tube will disappear, but if it is as low as 0.04 Hz (c), the desired signal will be oscillating and the result under steady-flow assumption (dotted line) is quite different from those in the oscillatory flow and under quasi-steady flow assumption. However, the result under quasi-steady flow assumption (dash-dotted line) is almost the same as that in the oscillatory flow (dashed line). It is confirmed that for the solute dispersion in an oscillatory flow, the mixing tube also acts as a low-pass filter, which is qualitatively consistent with the theoretical and experimental evidences for the solute dispersion in the steady flow in the microchannels [31].

3.4 Effect of the length of the mixing tube on the solute dispersion

Figure 6 shows the desired dynamic solute signals versus dimensionless time τ at the outlets of the mixing tube with different lengths (0.1, 0.2, 0.3 and 0.5 m, respectively) when both the frequencies of oscillatory flow and oscillatory solute concentration are set to 0.04 Hz. It is readily seen that as increases in the length of the mixing tube, the desired dynamic solute signals at the outlet have much more decay, which is in accordance with the conclusion in [31]. It is also evident that as the length of the mixing tube increases, the difference between the desired dynamic solute signals under steady flow assumption (dotted line) and those in the oscillatory flow (dashed line) and under quasi-steady flow assumption (dash-dotted line) will magnify although the result under quasi-steady flow assumption (dash-dotted line) is almost the same as that in the oscillatory flow (dashed line).

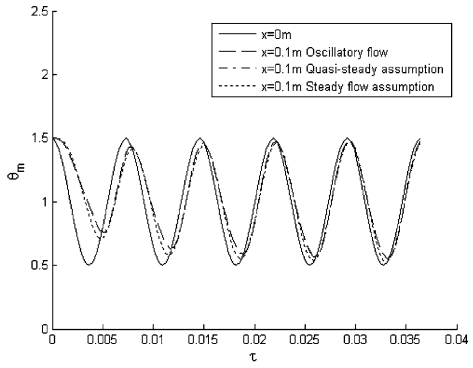

(a) $L = 0.1m$

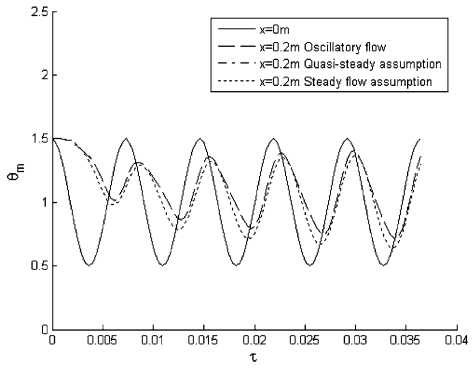

(b) $L = 0.2m$

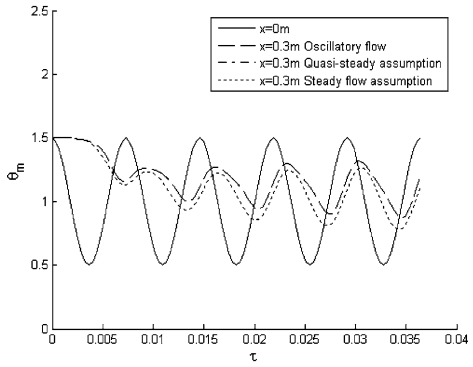

(c) $L = 0.3m$

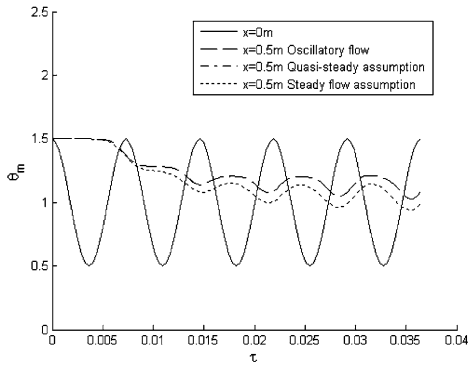

(d) $L = 0.5m$

Fig. 6 Effect of the length of the mixing tube on the dimensionless average concentration θ_m versus dimensionless time τ for $f = 0.04$ Hz and $f_\Omega = 0.04$ Hz

4 Discussion

The tube mixer as designed in Fig. 1 provides the possibility for simultaneously generating independent dynamic flow signals and biochemical signals at the outlet of the mixing tube. It is for the purpose of evaluating the effect of dispersion in an oscillatory flow on the desired dynamic biochemical signals, the expressions of the dispersion coefficients $K_1(\tau)$ and $K_2(\tau)$ are determined by using the

method of Gill and Sankarasubramanian [13], and an approximation equation governing the dimensionless average concentration θ_m in the mixing tube is obtained, which constitutes the main contribution of this paper.

In order to test the accuracy of quasi-steady flow assumption, the expressions of the dispersion coefficients $K_1(\tau)$ and $K_2(\tau)$ are simplified. The numerical simulation results show that the dispersion coefficients $K_1(\tau)$ and $K_2(\tau)$, and the desired dynamic solute signals at the outlet of the mixing tube under the quasi-steady flow assumption are almost the same as those calculated by using the original expressions in the oscillatory flow, demonstrating that the quasi-steady flow assumption can be used for the calculation of the dispersion coefficients $K_1(\tau)$ and $K_2(\tau)$, and the desired dynamic solute signals at the outlet of the mixing tube. It is interesting to test whether the steady flow assumption can be used to further simplify the calculation while still maintaining sufficient accuracy. The desired dynamic signals are also calculated by using the expressions of the dispersion coefficients $K_1(\tau)$ and $K_2(\tau)$ under the steady flow assumption. The numerical results show that when the frequency of oscillatory flow is high enough, e.g., $f = 1Hz$, which is similar to the fundamental frequency of human pulsatile blood flow in vivo, the steady flow assumption can be used for the determination of the desired dynamic solute signals.

The effects of the frequencies of oscillatory flow and oscillatory solute concentration on the solute dispersion are also analyzed. While the frequency of oscillatory flow doesn't seriously affect the solute dispersion (see Fig. 4), the solute dispersion is significantly dependent on the frequency of oscillatory solute concentration at the inlet (see Fig. 5). It is manifested that as increases in the frequency of oscillatory solute concentration in an oscillatory flow, the desired dynamic solute at the outlet of the mixing tube have much more decay, demonstrating that the mixing tube acts as a low-pass filter, which is consistent with the conclusion in [31].

The effect of the length of the mixing tube on the solute dispersion is also evaluated. It is concluded that as increases in the length of the mixing tube, the desired dynamic solute signals at the outlet have much more decay, which is also in accordance with the conclusion in [31]. It is also evident that as the length of the mixing tube increases, the difference between the desired dynamic solute signals under steady flow assumption and those in the oscillatory flow and under quasi-steady flow assumption will enlarge (see Fig. 6).

In summary, for the dispersion in an oscillatory flow, the dispersion coefficients $K_i(\tau)$ $(i = 1, 2)$ are determined as the functions of dimensionless time τ, and an approximation equation governing the dimensionless average concentration θ_m in the mixing tube is obtained. An excellent accuracy can be achieved by using quasi-steady flow assumption while the steady flow assumption would lead to inaccurate results. However, if the frequency of oscillatory flow is high enough, the steady flow assumption can be used to further simplify the calculation while still maintaining sufficient accuracy. These results are of practical importance in producing dynamic biochemical signals as the stimuli of biological cells by a tube mixer.

Acknowledgments The research reported here was supported by NUS Academic Research Fund R-263-000-483-112. The authors would like to thank the anonymous reviewers for their invaluable comments to improve the quality of this paper.

References

1. Ando J, Ohtsuka A, Korenaga R, Kamiya A (1991) Effect of extracellular ATP level on flow-induced Ca^{2+} response in cultured vascular endothelial cells. Biochem Biophys Res Commun 179:1192–1199
2. Aris R (1956) On the dispersion of a solute in a fluid flowing through a tube. Proc R Soc Lond A 235:67–77
3. Aris R (1960) On the dispersion of a solute in pulsating flow through a tube. Proc R Soc Lond A 259:370–376
4. Azizi F, Mastrangelo CH (2008) Generation of dynamic chemical signals with pulse code modulators. Lab Chip 8(6):907–912
5. Bandyopadhyay S, Mazumder BS (1999) On contaminant dispersion in unsteady generalised Couettee flow. Int J Eng Sci 37:1407–1423
6. Bandyopadhyay S, Mazumder BS (1999) Unsteady convective diffusion in a pulsatile flow. Acta Mech 134:1–16
7. Cegeaux JL, Grondelle AV (1997) Accuracy of the inverse Womersley method for the calculation of hemodynamic variables. Ann Biomed Eng 25(3):536–546
8. Chatwin PC (1973) On the longitudinal dispersion of dye whose concentration varies harmonically with time. J Fluid Mech 58(4):657–667
9. Chatwin PC (1975) On the longitudinal dispersion of passive contaminant in oscillatory flows in tubes. J Fluid Mech 71:513–527
10. Chen L, Azizi F, Mastrangelo CH (2007) Generation of dynamic chemical signals with microfluidic C-DACs. Lab Chip 7(7):850–855
11. Dull RO, Davies PF (1991) Flow modulation of agonist (ATP)-response Ca^{2+} coupling in vascular endothelial cells. Am J Physiol Heart Circ Physiol 261:H149–H154
12. Gill WN, Sankarasubramanian R (1970) Exact analysis of unsteady convective diffusion. Proc R Soc Lond A 316:341–350
13. Gill WN, Sankarasubramanian R (1971) Dispersion of a non-uniform slug in time-dependent flow. Proc R Soc Lond A 322:101–117
14. Gill WN, Sankarasubramanian R (1972) Dispersion of a non-uniformly distributed time-variable continuous sources in time-dependent flow. Proc R Soc Lond A 327:191–208
15. Hancock JT (1997) Cell signaling. Prentice-Hall, NY
16. Hazra SB, Gupta AS, Niyogi P (1996) On the dispersion of a solute in oscillating flow through a channel. Heat Mass Transf 31(4):249–256
17. Hazra SB, Gupta AS, Niyogi P (1997) On the dispersion of a solute in oscillating flow of a non-Newtonian fluid in a channel. Heat Mass Transf 32(6):481–487

18. Jiang Y, Grotberg JB (1993) Bolus contaminant dispersion in oscillatory tube flow with conductive walls. J Biomech Eng Trans ASME 115:424–431
19. Lin F, Saadi W, Rhee SW, Wang SJ, Mittal S, Jeon NL (2004) Generation of dynamic temporal and spatial concentration gradients using microfluidic devices. Lab Chip 4(3):164–167
20. Mo M, Eskins SG, Schilling WP (1991) Flow-induced changes in Ca^{2+} signaling of vascular endothelial cells: effect of shear stress and ATP. Am J Physiol Heart Circ Physiol 260:H1698–H1707
21. Mukherjee A, Mazumder BS (1988) Dispersion of contaminant in oscillatory flows. Acta Mech 74:107–122
22. Ng CO (2004) A time-varying diffusivity model for shear dispersion in oscillatory channel flow. Fluid Dyn Res 34:335–355
23. Ng CO (2006) Dispersion in steady and oscillatory flows through a tube with reversible and irreversible wall reaction. Proc R Soc Lond A 462:481–515
24. Olofsson J, Bridle H, Sinclair J, Granfeldt D, Sahlin E, Orwar O (2005) A chemical waveform synthesizer. PNAS 102(23):8097–8102
25. Palsson BO, Bhatia SN (2004) Tissue engineering. Prentice-Hall, NY
26. Qin KR, Xiang C, Xu Z, Cao LL, Ge SS, Jiang ZL (2008) Dynamic modeling for shear stress induced ATP release from vascular endothelial cells. Biomech Model Mechanobiol 7(5):345–353
27. Smith R (1982) Contaminant dispersion in oscillatory flows. J Fluid Mech 114:379-398
28. Taylor GI (1953) Dispersion of soluble matter in solvent flowing slowly through a tube. Proc R Soc Lond A 219:186–203
29. Wolpert L, Beddington R, Jessell TM, Lawrence P, Meyerowitz EM, Smith J (2002) Principles of development. Oxford, NY
30. Womersley JR (1955) Method for the calculation of velocity, rate flow, and viscous drag in arteries when the pressure gradient is known. J Physiol 127(3):553–563
31. Xie Y, Wang Y, Chen L, Mastrangelo CH (2008) Fourier microfluidics. Lab Chip 8(5):779–785
32. Yamamoto K, Korenaga R, Kamiya A, Ando J(2000) Fluid shear stress activates Ca^{2+} influx into human endothelial cells via $P2X_4$ purinoceptors. Circ Res 87:385–391
33. Yasuda H (1984) Longitudinal dispersion of matter due to the shear effect of steady and oscillatory currents. J Fluid Mech 148:383–403